

The survival of dynamical fossils in dwarf spheroidal galaxies in conventional and modified dynamics

F. J. Sánchez-Salcedo^{1*} and V. Lora^{1,2}

¹*Instituto de Astronomía, Universidad Nacional Autónoma de México, P.O. Box 70-264, C.P. 04510, Mexico City, Mexico*

²*Astronomisches Rechen-Institut, Zentrum für Astronomie der Universität Heidelberg, Mönchhofstr. 12-14, 69120 Heidelberg, Germany*

Accepted xxxx Month xx. Received xxxx Month xx; in original form 2009 December 10

ABSTRACT

The survival of unbound density substructure against orbital mixing imposes strong constraints on the slope of the underlying gravitational potential and provides a new test on modified gravities. Here we investigate whether the interpretation that the stellar clump in Ursa Minor (UMi) dwarf spheroidal galaxy is a ‘dynamical fossil’ is consistent with Modified Newtonian dynamics (MOND). For UMi mass models inferred by fitting the velocity dispersion profile, the stellar clump around the second peak of UMi is erased very rapidly, within 1.25 Gyr (6.5 orbits), even with the inclusion of self-gravity. We find that the clump can hardly survive for more than 2 Gyr even under more generous conditions. Alternative scenarios which could lead to a kinematically cold clump are discussed but, so far, none of them were found to be fully satisfactory. Our conclusion is that the cold clump in UMi poses a challenge for both Λ CDM and MOND.

Key words: galaxies: individual (Ursa Minor dSph) – galaxies: kinematics and dynamics – dark matter – gravitation – stellar dynamics

1 INTRODUCTION

The standard concordance cosmological model with cold dark matter (Λ CDM model) is remarkably successful on scales larger than 1 Mpc, but it faces challenges on smaller scales. For instance, it seems that the theory predicts a too cuspy density profile for the dark matter at the centres of galaxies (e.g., Trachternach et al. 2008). The Modified Newtonian Dynamics (MOND) proposed by Milgrom (1983) has proven to be successful in reproducing the kinematics of spiral galaxies without any assumption of unseen matter (see Sanders & McGaugh 2002, for a review), from extremely low mass galaxies of low surface brightness (Milgrom & Sanders 2006) to high luminosity galaxies (Sanders & Noordermeer 2007). Gentile et al. (2007) found that the observed rotation curves in tidal dwarf galaxies are quite naturally explained without any free parameters within MOND, and are inconsistent with the current Λ CDM theory (see also Kroupa et al. 2005). If MOND is able to naturally account for all of the discrepancies faced by Λ CDM on small scales, this would lend strong support to MOND.

In the Newtonian dark matter scenario, dwarf spheroidal galaxies (dSph’s) require the largest mass-to-light ratios. Hence, dSph’s provide a unique testing ground for the nature of dark matter and its alternatives (Gerhard &

Spiegel 1992; Milgrom 1995; Lokas et al. 2006; Sánchez-Salcedo et al. 2006; Angus 2008). However, the mass-to-light ratios inferred in MOND are very sensitive to uncertainties on the structural parameters, luminosities, distances and internal velocity dispersions. It is, therefore, important to explore other gravitational effects, which, in principle, may offer independent tests.

In the dark matter paradigm, the velocity dispersion profiles of the brightest dSphs are consistent with both a cuspy NFW halo and a cored dark halo. However, there exists some indirect evidence that dSph galaxies may possess a core (Kleyna et al. 2003, hereafter K03; Goerdt et al. 2006; Sánchez-Salcedo et al. 2006). In particular, K03 considered the survival of the cold density substructure detected in photometric data in Ursa Minor (UMi). This substructure appears as an off-centre localized stellar clump with low velocity dispersion $\simeq 0.5 \text{ km s}^{-1}$. K03 concluded that the secondary peak in UMi is a long-lived structure, surviving in phase-space because the underlying gravitational potential is close to harmonic. In the standard dark matter paradigm, this implies that the dark matter halo in UMi must have a large core because, if the dark halo has a central density cusp, the clump should have diluted in ~ 1 Gyr. Even if dSph galaxies are influenced to some degree by the tidal forces exerted by the Milky Way, it is unlikely that such a large core may have a tidal origin (e.g., Stoehr et al. 2002; Hayashi et al. 2003; Peñarrubia et al. 2008). It is worthwhile

* E-mail: jsanchez@astroscu.unam.mx

exploring if the competing MOND scenario can explain the survival of cold substructures in dSph galaxies in a natural way. The question that arises is whether the MOND gravitational potential can mimic the potential of a dark halo with a core in order to explain the very longevity of the dynamical fossil in UMi. In other words, can the inference of cored haloes in dSphs be accommodated naturally within MOND?

This paper is organized as follows. In section 2, we give a general statement of the problem and outline some key analytic results for tidal dissolution of satellite systems. In section 3, we briefly describe the observational properties of UMi dwarf and its clump. Some important issues regarding the assumptions and approximations made to study the evolution of the clump in MOND framework are given in section 4. Section 5 presents results on the evolution of a stellar clump in MOND. In section 6, we discuss alternative scenarios to account for the persistence of kinematically cold substructure in dSph galaxies. Finally, our conclusions are summarized in section 7.

2 EVOLUTION OF SATELLITE SYSTEMS AND UNBOUND CLUMPS: TIDAL RADIUS AND EPICYCLIC THEORY

Suppose that a small clump of mass M_{cl} is on a circular orbit with radius R_{cir} around its host galaxy, which is assumed to be spherical. If the circular speed with which a test particle orbits in the gravitational potential of the host galaxy can be described by a power-law $v_c^2 \propto r^l$ with $-1 \leq l \leq 2$, the tidal radius is given by

$$r_t = k \left[\frac{\chi_{cir}}{2-l} \right]^{1/3} R_{cir}, \quad (1)$$

where χ_{cir} is the ratio between the mass of the clump and the mass of the host galaxy mass inside R_{cir} , and k is Keenan’s (1981a,b) factor, which accounts for the elongation of the zero-velocity surface along the line joining the clump and the centre of the host galaxy. For the Keenan factor, we will take the nominal value $k = 1$ (see section 2 in Sánchez-Salcedo & Hernandez 2007 for a discussion). Zhao (2005) and Zhao & Tian (2006) showed that the expression for the dynamical tidal radius given in Eq. (1) is also valid in MOND as long as χ_{cir} is taken as the ratio between the “true” baryonic masses of the satellite and the host galaxy (see Sánchez-Salcedo & Hernandez 2007 for a discussion). We see from Eq. (1) that it may happen that the clump is essentially unbound ($M_{cl} \rightarrow 0$ and $\chi_{cir} \rightarrow 0$), but it is not dissolved because $l \rightarrow 2$. This is true in both Newtonian and MOND gravity. The case $l = 2$ corresponds to the harmonic potential. If the potential is quasi-harmonic, the orbital period depends weakly on the energy of the stars and hence the phase mixing is highly suppressed even if self-gravity of the clump is ignored.

Much of early work on the dynamics of unbound satellites used the epicycle theory to describe their evolution (e.g., Oort 1965; Wielen 1977; Fellhauer & Heggie 2005). From the linear epicyclic theory, we learn that it is possible to prepare a small unbound system with a nonzero velocity dispersion that will orbit with almost no secular spreading (e.g., Kuhn 1993). In fact, in an idealized situation where all the stars of the clump have the same guiding centre, the clump would preserve its original size in the epicyclic

approximation because the epicycle and orbital frequencies are the same for all stars. However, even if we start with a very idealized situation in which all the stars of the clump move on retrograde orbits resembling epicycles with a common guiding centre, self-gravity of the clump destroys the coherent stellar motions and the dissolution time is infinite only when the density of the clump is negligible. Fellhauer & Heggie (2005) studied the time of dissolution of such unbound stellar system, in Newtonian gravity, as a function of its initial internal density and size. They found that a system orbiting within a galaxy modeled as an isothermal sphere, can survive for about 10 galactic orbits only if it has a very low density ($\sim 5\%$ of the background density) and small radius (0.5% of the orbital radius). For larger internal densities of the clump, the dissolution becomes more rapid. In the Appendix A, we extend the theoretical analysis of Fellhauer & Heggie (2005) to MOND gravity. We consider a small unbound clump orbiting on a circular orbit around the centre of a galaxy. It is shown that, because of the enhanced self-gravity in MOND, the dissolution time of a certain unbound clump is shorter in MOND than in its equivalent Newtonian galaxy, that is, the Newtonian galaxy (the same distribution of stars plus additional dark matter) which has the same “dynamics” as the MOND galaxy.

3 URSA MINOR AND ITS DYNAMICAL FOSSIL

3.1 UMi: Structural parameters

Ursa Minor is located at a heliocentric distance of $D = 76 \pm 4$ kpc (Carrera et al. 2002; Bellazzini et al. 2002). The star formation history and the characteristics of the population of blue straggler stars suggest that UMi is a truly ‘fossil’ galaxy, where star formation ceased completely more than 8 Gyr ago (Carrera et al. 2002; Mapelli et al. 2007). The shape of the inner isodensity contours of the surface density of stars appears to be elliptical with a large ellipticity ($\epsilon = 0.54$). The King core radius of the stellar component along the semimajor axis is $17.9'$ (~ 395 pc at 76 kpc) (Palma et al. 2003).

In the Newtonian dark matter scenario, values for M/L_V ranging between 30 to 200 can be inferred depending on the adopted global luminosity, distance and velocity dispersion profile. In particular, if we rescale the results of Gilmore et al. (2007) for $D = 76$ kpc and use the updated luminosity of $L_V = 1.1 \times 10^6 L_\odot^V$ (Palma et al. 2003), the total mass within 0.6 kpc is $\gtrsim 7 \times 10^7 M_\odot$, resulting in a $M/L_V \gtrsim 64 M_\odot/L_\odot^V$. If we use the dispersion profile of Muñoz et al. (2005), the M/L_V is reduced by a factor ~ 2 .

3.2 The secondary peak of UMi revisited

Several authors have reported structure in the surface density of UMi on a variety of scales (Olszewski & Aaronson 1985; Demers et al. 1995; Irwin & Hatzidimitriou 1995; Kleyna et al. 1998; Eskridge & Schweitzer 2001; Palma et al. 2003). The most remarkable feature is the double off-centered peak in the stellar surface number density. In this paper, we concentrate on the secondary peak, observed on the northeastern side of the major axis of UMi.

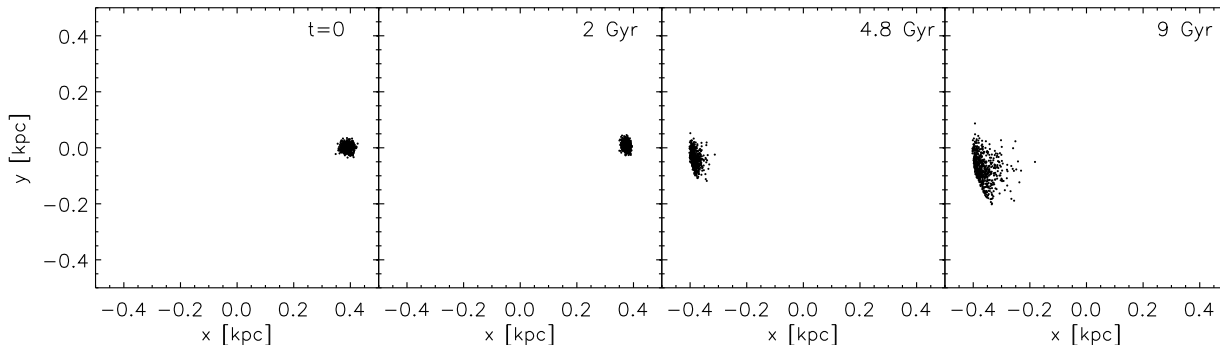


Figure 1. Snapshots of an unbound clump at $t = 0, 2, 4.8$ and 9 Gyr in a dark matter halo with a scale radius R_s equal to 2.4 times the semimajor axis of the size of clump’s orbit. The clump has an initial 1σ radius of 12 pc, one-dimensional velocity dispersion of 0.5 km s^{-1} and a speed at apogalacticon equal to 0.07 times the circular speed.

K03 found that the radius of the clump is $\gtrsim 6'$ (equivalent to 135 pc at $D = 76$ kpc); this is the largest circle where the isophlet contours indicate the presence of a secondary peak in the stars. The velocity of stars that form the secondary peak is best fitted by a two-Gaussian population, one representing the 8.8 km s^{-1} Gaussian background and the other representing a cold subpopulation of 0.5 km s^{-1} velocity dispersion. The cold group of stars has the same mean velocity as the systematic velocity of UMi, so it is likely that its orbit is close to the plane of the sky.

The luminosity bump can be fitted approximately by a Gaussian density profile $\rho = \rho_0 \exp(-r'^2/2r_0^2)$, where r' is the radial distance to the peak in the stars, and $r_0 \simeq 35$ pc (e.g., Palma et al. 2003). The projected surface density of the clump along its centre is: $\sqrt{2\pi}\rho_0 r_0$. Since the underlying stellar population of UMi also contributes to the observed surface density, we need the fraction f of stars that belongs to the kinematically cold subpopulation. K03 found that the subpopulation fraction is $f = 0.7$ in the best fit. Equating $\sqrt{2\pi}\rho_0 r_0$ with f times the observed surface density at the secondary peak, we can infer ρ_0 and then the total mass in the clump $M_{cl} \simeq 16\rho_0 r_0^3$. Using $f = 0.7$, we obtain

$$M_{cl} = 7.8 \times 10^4 M_\odot \left(\frac{\Upsilon_\star}{5.8} \right), \quad (2)$$

where Υ_\star is the V band mass-to-light ratio of UMi stellar population. For a normal stellar population $\Upsilon_\star \approx 2$, we have $M_{cl} = 2.5 \times 10^4 M_\odot$.

An inspection of the stellar isophlets in UMi suggests that the secondary peak is unbound material because of its large angular size in the plane of the sky, as compared to the expected value for a bound cluster, and its bend in the isodensity contours, indicative of tidal disruption (Palma et al. 2003). Let us estimate the tidal radius of a stellar cluster of mass $M_{cl} = 2.5 \times 10^4 M_\odot$, as UMi’s clump, on a circular orbit in a galaxy with a flat rotation curve at R_{cir} (i.e. $l = 0$ in Eq. 1). For a UMi-like galaxy, the mass interior to $R_{cir} = 390$ pc in the standard dark matter scenario is $\simeq 10^7 M_\odot$. According to Eq. (1), the clump would remain gravitationally bound only if all the mass that comprises the stellar cluster were placed within a sphere of 42 pc radius. The appearance of such a hypothetical cluster should resemble a globular cluster as those detected in Fornax dSph

galaxy and, therefore, easily detectable as a distinct spherical bound object. This is not the case for the secondary peak in UMi and, thus, it turns out that the clump is unbound at least in the dark matter scenario.

Since there is no evidence that the regions of density excess have stellar populations that differ from the main body of UMi (Kleyna et al. 1998), the most plausible interpretation is that this density structure, or clump, is a disrupted stellar cluster (K03; Read et al. 2006; section 6). K03 argues that the persistence of a dynamically separate unbound entity for $10 - 12$ Gyr, is possible only if the background potential is quasi-harmonic (see section 2), implying that the dark halo has a large core. For illustration, Figure 1 shows the evolution of a clump made of test particles, orbiting in a spherical dark halo with a density mass profile of the form

$$\rho_{dm}(r) = \frac{\rho_{max}}{(1 + [r/R_s]^2)^{1/2}}, \quad (3)$$

where R_s is the scale radius. Following K03, the central density ρ_{max} was selected such that the circular velocity is 19 km s^{-1} at an angular distance of $31.5'$, i.e. at ~ 700 pc. The contribution of the stellar mass to the gravitational potential was ignored because its mass interior to 0.4 kpc ($0.9 \times 10^6 M_\odot$) is only 9%, or less, of the dark matter mass, if we assume that UMi has a normal stellar V -band mass-to-light ratio of $\sim 2M_\odot/L_{V,\odot}$. The clump was dropped at a distance $R_s/2.4$ on a near radial orbit with a tangential velocity equal to 0.07 times the circular velocity at its initial position. The clump has initially a 1σ radius of 12 pc and one-dimensional velocity dispersion of 0.5 km s^{-1} , similar to those selected by K03 in order to facilitate comparison. The orbit lies in the (x, y) -plane. From Figure 1, we see that, although the density structure becomes more extended over time, it may survive for many Gyr if we assume that the scale radius of the dark halo is at least 2–3 times the size of clump’s orbit, confirming K03 results. Due to the phase mixing, those components of the velocity dispersion along the orbital plane (i.e. σ_x and σ_y) increase with time, whereas the perpendicular component to the orbital plane remains constant. As a consequence, the size of the clump does not increase along the axis perpendicular to the orbital plane, and remains dynamically cold in that direction ($\sigma_z \simeq 0.5$ km s^{-1}).

Lora et al. (2009) have simulated the dynamics of a clump including self-gravity. They show that density substructure can persist for ~ 12 Gyr in a halo with a scale radius equal to 1.5 times the size of the clump's orbit. Assuming that the size of the orbit is ~ 390 pc, a scale radius for the dark halo of $R_s = 1.5 \times 390$ pc = 580 pc is required. Note that R_s was defined as the radius at which the density has dropped a factor $\sqrt{2}$. This large core is at odds with the predictions of Λ CDM. Therefore, the interpretation that the clump survives because the gravitational potential is quasi-harmonic poses a challenge to the standard Λ CDM, which predicts cuspy NFW profiles. In the next sections, we investigate whether MOND can account for the survival of the clump.

4 THE CASE OF MOND: CONCEPTS AND APPROXIMATIONS

In MOND, the luminous density profile determines the shape of the gravitational potential and, thus, the index l in Eq. (1). Moreover, χ_{cir} is not sensitive to the adopted stellar mass-to-light ratio as soon as we assume that the stellar mass-to-light ratio of the clump is similar to that of the stellar bulk of UMi. Consequently and according to Eq. (1), the tidal radius is very robust to the adopted stellar mass-to-light ratio. Since the only free parameter is, in principle, the stellar mass-to-light ratio, the survival of the clump in UMi is an interesting dynamical test to MOND. We must warn here that Eq. (1) was derived for MOND satellite systems embedded in *isolated* host galaxies. As it will become clear later, UMi is affected by the Galactic field and cannot be treated as it was in isolation.

In MOND framework, the gravitational potential describing the force acting on a star in UMi obeys the modified Poisson equation of Bekenstein & Milgrom (1984)

$$\nabla \cdot (\mu(x)\nabla\Phi) = 4\pi G\rho, \quad (4)$$

where $x = |\nabla\Phi|/a_0$, $a_0 \simeq 1.2 \times 10^{-8}$ cm s $^{-2}$ is the universal acceleration constant of the theory and $\mu(x)$ is the interpolating function which runs smoothly from $\mu(x) = x$ at $x \ll 1$ to $\mu(x) = 1$ at $x \gg 1$. Equation (4) must be solved with the boundary condition $\nabla\Phi \rightarrow -\mathbf{g}_E$, where \mathbf{g}_E is the external gravity acting on UMi, which has a magnitude $g_E = V^2/R_{gc}$, where V is the Galactic rotational velocity at R_{gc} , which coincides with the asymptotic rotation velocity V_∞ for the Milky Way. Although V_∞ is very difficult to determine observationally in our Galaxy, Famaey & Binney (2005) and Sánchez-Salcedo & Hernandez (2007) argue that it must be of 170 ± 5 km s $^{-1}$ by adopting a mass model for the Milky Way under MOND.

A clump star feels the external acceleration created by the Milky Way (\mathbf{g}_E), the acceleration generated by UMi background stars (\mathbf{g}_I) and the acceleration generated by all the other stars of the clump (\mathbf{g}_{int}). Due to the non-linearity of the MOND field equation, the gravitational acceleration \mathbf{g}_I is altered by the gravitational field of the Milky Way, whereas \mathbf{g}_{int} is altered by both \mathbf{g}_E and \mathbf{g}_I .

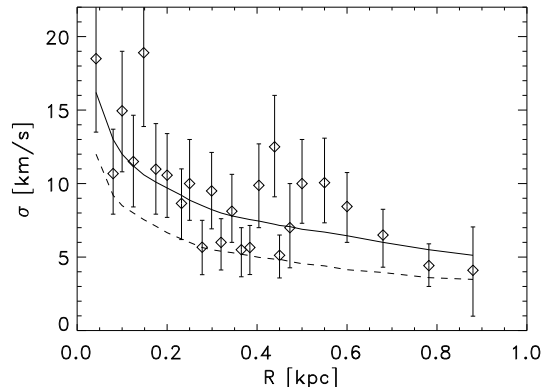


Figure 2. The observed UMi line-of-sight velocity dispersion versus projected radius is shown as diamonds with errorbars. The solid line corresponds to the best fitting model in MOND ($Y_\star = 5.8$) and the dashed line shows the predicted velocity dispersion for $Y_\star = 2.2$, which is at 1σ from the best fitting value.

4.1 Modelling UMi background gravitational potential under MOND

Only for very special configurations (one-dimensional symmetry –spherical, cylindrical or plane symmetric systems– or Kuzmin discs) the MOND acceleration \mathbf{g} is related to the Newtonian acceleration, \mathbf{g}_N , by the algebraic relation $\mu(|\mathbf{g}|/a_0)\mathbf{g} = \mathbf{g}_N$ (Brada & Milgrom 1995). Milgrom (1986) showed that when the mass distribution involves a small perturbation in a medium under a uniform external field, the perturbation in the gravitational potential satisfies an *anisotropic* Poisson-like equation with a dilation along z , which is taken as the direction of the external field \mathbf{g}_E (see the Appendix A). For instance, the ‘modified’ Plummer model for a satellite of mass M in this quasi-Newtonian limit is (e.g., Sánchez-Salcedo 2009):

$$\rho_p(\mathbf{r}) = \rho_c \left[1 + \frac{x^2 + y^2}{r_p^2} + \frac{z^2}{(1 + L_0)r_p^2} \right]^{-5/2}, \quad (5)$$

$$\Phi_p(\mathbf{r}) = -\frac{1}{\mu_0} \frac{GM}{\sqrt{(1 + L_0)(x^2 + y^2) + z^2 + \bar{r}_p^2}}, \quad (6)$$

where

$$\rho_c = \frac{3M}{4\pi(1 + L_0)^{1/2}r_p^3}, \quad (7)$$

r_p and $\bar{r}_p \equiv (1 + L_0)^{1/2}r_p$ are the characteristic radii and L_0 is the logarithmic derivative of $\mu_0 \equiv \mu(g_E/a_0)$ and hence $0 \leq L_0 \leq 1$. This pair is solution of the hydrostatic Jeans equation for an isotropic velocity dispersion tensor. We see that the potential becomes Newtonian, but with a larger effective gravitational constant $\mu_0^{-1}G$, and anisotropic. In the case of halo objects at distances D much larger than the galactocentric distance of the Sun ~ 8 kpc, the direction of the external field from the Milky Way almost coincides with the line-of-sight.

As an approximation and effective way to take into account the external field effect (EFE) in dSph galaxies, Angus (2008) used the following relation between the internal \mathbf{g}_I and external \mathbf{g}_E accelerations:

$$\mathbf{g}_I \mu(x) = \mathbf{g}_N, \quad (8)$$

where \mathbf{g}_N is the Newtonian internal acceleration of the subsystem and $x = \sqrt{g_I^2 + g_E^2}/a_0$. In view of the success of the model in reproducing the kinematics of the classical dSph galaxies (Angus 2008), we will use Eq. (8) to derive \mathbf{g}_I . As we will see in the following, Equation (8) is interpreted as one of the simplest way to interpolate between the isolated and the quasi-Newtonian regimes. Due to its simplicity, it has proven to be very useful to treat the EFE (e.g., Wu et al. 2007; Angus & McGaugh 2008; see also Llinares et al. 2008). At locations where $g_I \gg g_E$, $x \simeq g_I/a_0$ and Eq. (8) can be simplified to the algebraic relation $\mu(g_I/a_0)\mathbf{g}_I = \mathbf{g}_N$, which is the exact solution of the Bekenstein-Milgrom equation if the subsystem is spherical or cylindrical (and it is a good approximation in other geometries like axisymmetric exponential discs, e.g., Brada & Milgrom 1995). In the opposite regime, i.e. in the quasi-Newtonian limit, where the dynamics is dominated by the external field, that is $g_E \gg g_I$, Eq. (8) can be written as $\mu(g_E/a_0)\mathbf{g}_I = \mathbf{g}_N$. Thus this approximation recovers the quasi-Newtonian dynamics predicted in linear theory, but does not capture the anisotropic dilation along the external field direction.

Suppose that we have a stellar clump embedded in an ellipsoidal potential, such as those described by Eq. (6). This flattened potential creates a torque on our clump, when the orbital plane of the clump is misaligned with the instantaneous direction of the external field (Wu et al. 2007). This causes additional orbital mixing that contribute to the dissolution of unbound clumps. Since the approximation of Eq. (8) cannot capture dilation, it neglects this source of orbital mixing. A more refined model to include the EFE dilation is not warranted, due to our ignorance about the density mass profile of UMi along the line of sight.

Angus (2008) used Jeans analysis to model the UMi velocity dispersion profile versus circular radii (rather than elliptical radii) reported in Muñoz et al. (2005) under MOND and demonstrated that the best-fit model for UMi's velocity dispersion is very reasonable. Therefore, we will adopt exactly the same parameters for UMi as in Angus (2008), which are compiled in our Table 1. The mass density of UMi was modelled by a spherical King model with a core radius of $17.9'$, which corresponds to the core radius along the semimajor axis. The velocity anisotropy was taken variable but the fit turned to be quite compatible with a constant anisotropy of 0.7. Figure 2 shows the observed velocity dispersion from Muñoz et al. (2005), together with the best MOND fit ($\Upsilon_\star = 5.8$, where again Υ_\star denotes the stellar V -band mass-to-light ratio in solar units), as well as the predicted MOND velocity dispersion profile when the 1σ error in Υ_\star is considered ($\Upsilon_\star = 2.2$)¹.

In the best fitting model, the circular velocity of a test particle at the stellar core radius ($r_c = 395$ pc) of UMi is ~ 13 km s⁻¹ (see Fig. 3). Therefore, the characteristic internal acceleration, $[v_c(r_c)]^2/r_c \simeq 0.14 \times 10^{-8}$ cm s⁻², is much smaller than $a_0 \simeq 1.2 \times 10^{-8}$ cm s⁻². On the other hand, the external acceleration, $V_\infty^2/R_{gc} \simeq 0.12 \times 10^{-8}$ cm s⁻², is

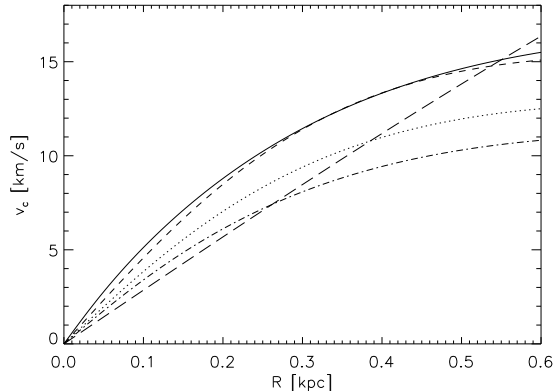


Figure 3. Circular speed curves for different models of UMi. For the reference MOND model, which has $\Upsilon_\star = 5.8$, the solid line shows the MOND rotation curve, whereas the short dashed line gives the Newtonian circular speed multiplied by a factor 2.5 to show that both curves almost match. Also shown is the rotation curve for a model with the same parameters than the reference model but with $\Upsilon_\star = 2.2$ (dot-dashed line). The dotted line gives the circular speed in the reference case ($\Upsilon_\star = 5.8$) but when the external field strength is doubled. For comparison, the rotation curve in Newtonian gravity with the dark matter halo described in section 3.2 is also plotted (long dashed line).

also much smaller than a_0 . We conclude that UMi internal dynamics lies in the deep-MOND regime and thus it is not sensitive to the exact form of the interpolating function. The ratio between the internal acceleration at UMi's core radius r_c and the external acceleration is a good measure of the importance of EFE. For our reference parameters given in Table 1, this ratio is ≈ 1.1 , which implies that UMi dSph galaxy is at an intermediate regime; it can be considered neither as isolated nor as external field dominated.

4.2 Self-gravity of the clump

We may define the internal acceleration \mathbf{g}_{int} of a clump's star as $\mathbf{g}_{\text{int}} = -\nabla\Phi - \mathbf{g}_E - \mathbf{g}_I$. In fact, the clump is embedded in the external field generated by all the other particles of UMi and the Milky Way. Due to the EFE, \mathbf{g}_{int} depends on both accelerations \mathbf{g}_E and \mathbf{g}_I . Suppose for a moment that the clump was spherical and seated at the centre of UMi. Since g_I is small compared to g_E in the centre of UMi, we should recover an equation identical to Eq. (8) for \mathbf{g}_{int} , i.e.

$$\mathbf{g}_{\text{int}} \mu(x) = \mathbf{g}_{\text{int},N}, \quad (9)$$

where $x = \sqrt{g_{\text{int}}^2 + g_E^2}/a_0$ and $\mathbf{g}_{\text{int},N}$ is the Newtonian internal acceleration of a star in the clump. If the clump is displaced at those distances from the centre of UMi where g_I is not longer negligible relative to g_E , Equation (9) overestimates clump's self-gravity, making it more resilient to tidal destruction.

At $g_{\text{int}} \gg g_E$, Equation (9) is the solution of the modified Poisson equation when our clump is spherical. Therefore, Equation (9) is valid provided that the mass density distribution of the clump is close to spherical at $g_{\text{int}} \gg g_E$. As time goes by, the clump and its tidal debris will form a non-spherical mass configuration because the stars lost from

¹ The discrepant values for Υ_\star between Angus (2008) and Sánchez-Salcedo & Hernandez (2007) is traced to the different distance, luminosity and velocity dispersion profile used (see section 3.1).

Table 1. A summary of relevant parameters for the reference model.

UMi	D kpc	L_V $10^5 L_{\odot,V}$	r_c pc	M $10^5 M_{\odot}$	M/L_V	$M(< r_c)$ $10^5 M_{\odot}$	$v_c(r_c)$ km s^{-1}	g_E/a_0	g_I/g_E at r_c
	76	11.0	395	63.5	5.8	26.0	13.2	0.1	1.15
Clump	semimajor axis in kpc ^a	L_V $10^5 L_{\odot,V}$	R_h pc	M $10^5 M_{\odot}$	M/L_V	χ_{cir}	$v_c(R_h)$ km s^{-1}	g_{int}/g_E at R_h	
	0.39	0.13	55	0.78	5.8	0.030	4.5 ^b	1.0	

^a It refers to the semimajor axis of orbit's clump. ^b This is the MOND prediction (not necessarily supported by observations –see text–).

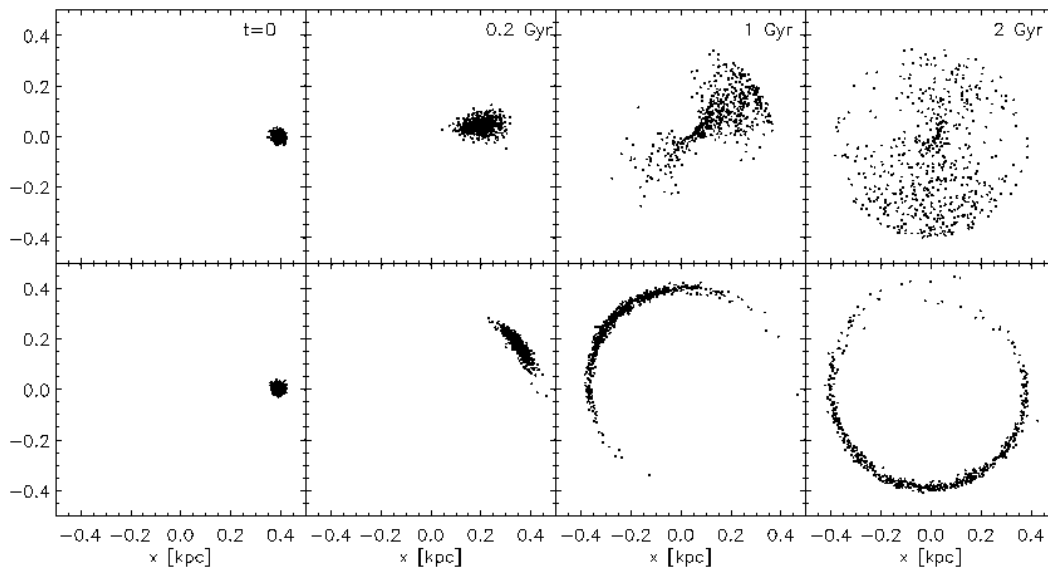


Figure 4. Evolution of a clump in the reference MOND model for a near radial orbit (top panels) and on a circular orbit (bottom panels) when clump’s self-gravity is ignored. The orbital plane of the clump lies in the (x, y) plane. Times since the start of the simulation are indicated.

the clump will form two tidal tails, one leading the clump and one trailing it. However, the break of spherical symmetry does not represent a real limitation because, as we will see in the next section, g_{int} is comparable to g_E only at the very beginning of the simulations when the clump is roughly spherical. In fact, internal accelerations of the order of g_E only occur at initial times and inside the clump, where the mass distribution can be considered as spherical.

In order to quantify the role of self-gravity, we will carry simulations in which the self-gravity is turned off (non-selfgravitating case, NSG) and simulations in which self-gravity is included through Eq. (9). According to the ongoing discussion, these are the limits of what can be expected

in MOND; the survival times derived with Eq. (9) represent upper values. In the remainder of the paper, we will refer to Eq. (9) as the reduced EFE approximation (REFE). Direct N-body simulations of 1200 particles were carried out using the code described in Lora et al. (2009) with the REFE approximation. The convergence of the results was tested by comparing runs with different softening radii and number of particles.

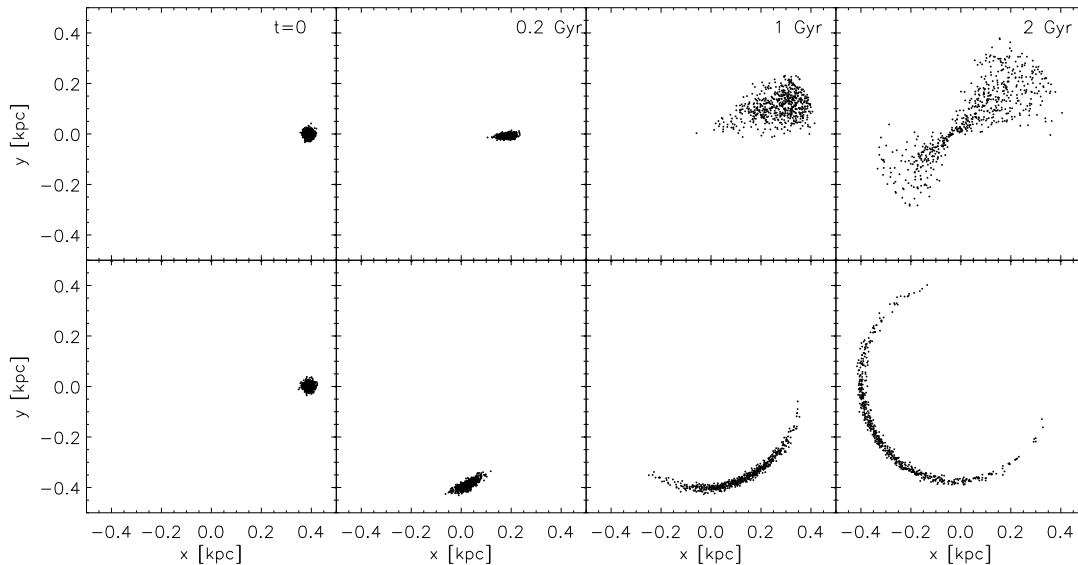


Figure 5. Same as Figure 4 but for a MOND model with $\Upsilon_* = 2.2$.

5 EVOLUTION OF A STELLAR CLUMP

5.1 NSG simulations

We consider first the reference model in which $\Upsilon_* = 5.8$. Figure 4 shows the disintegration of a NSG clump on a near radial orbit with an apogalactic distance of 390 pc and on a circular orbit with a radius of 390 pc. In the case of a near radial orbit, the clump was dropped at apogalacticon with a tangential velocity equal to 0.07 the local circular velocity. The initial 1σ radius of 12 pc and velocity dispersion of the stars in the clump of 0.5 km s^{-1} are the same as those used in section 3.2. Phase mixing dissolves the clump very rapidly; the clump doubles its size in 0.2 Gyr (essentially one orbital revolution of the clump about UMi) and it becomes completely diluted in less than 1.25 Gyr (~ 6.5 orbital periods). When the clump is on a circular orbit, the tidal debris populates the whole ring of the orbit, due to the effect of differential rotation. The clump is shortlived because the MOND circular velocity $v_c(r)$ of UMi is essentially a scaled-version of the Newtonian (without dark matter) circular velocity at $r < 0.6 \text{ kpc}$ (see Fig. 3). Thus, the evolution of the clump in MOND resembles that in a purely Newtonian galaxy with a dark halo having a core equal to r_c , i.e. a mass-follows-light model. Since the core radius of the fictitious dark halo is almost equal to the clump's orbit, the group of stars is erased in a few crossing times. In other words, MOND is not able to change significantly the shape of the gravitational potential within the orbit of the clump, at least not enough to generate a near-isochrone potential needed to guarantee the survival of the clump.

Since the destruction time roughly scales as the galactic crossing time for the clump, one can increase the longevity of the clump by decreasing the mass of UMi if a lower mass-to-light ratio of the stellar population of UMi is adopted. Figure 5 shows the evolution of the same clump if the body of the stars in UMi has $\Upsilon_* = 2.2$. The clump is diluted in $< 2 \text{ Gyr}$. Even when using a M/L_V value seven times smaller than the preferred mass-to-light ratio (i.e. $\Upsilon_* = 0.83$) and the clump is initialized with a velocity dispersion of 0.25 km s^{-1} , the group of stars dissolves in $< 2.5 \text{ Gyr}$ (see Fig. 6). Values for the mass-to-light ratio below 0.83 may be problematic because then UMi may be too fragile to the process of tidal disruption.

Similarly, the survival time can also be enhanced by assuming a larger value for the external field acceleration g_E . When we double the strength of the external field in our reference model, the clump still dissipates in $< 2 \text{ Gyr}$. For comparison, the circular speed for this model was also plotted in Fig. 3. The uncertainty on V_∞ cannot change significantly the disruption timescale. Doubling g_E corresponds to an asymptotic circular velocity of 250 km s^{-1} , which sounds unrealistic in MOND.

5.2 Simulations with self-gravity

In the previous section, we have considered the fate of an unbound clump in MOND. Even if the clump is initially very compact (a 1σ radius of 12 pc), orbital phase mixing dilutes the overdensity structure within less than 2 Gyr in MOND models. When self-gravity of the clump is included, a clump

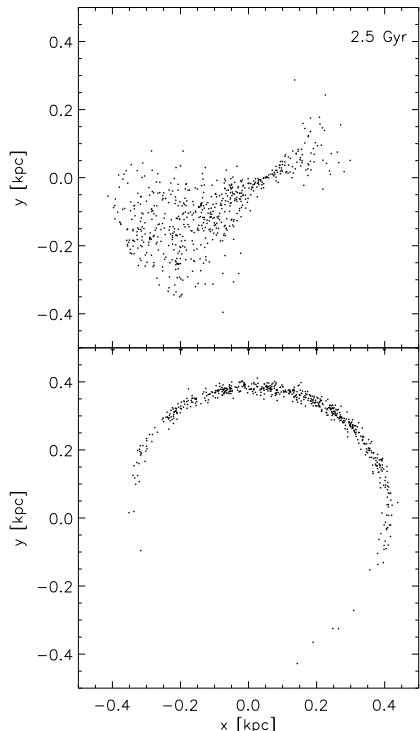


Figure 6. Distribution of the stellar debris projected onto the orbital plane at $t = 2.5$ Gyr in a MOND case with $\Upsilon_\star = 0.83$, when the clump with initial velocity dispersion of 0.25 km s^{-1} is on a near radial orbit (upper panel) and on a circular orbit (bottom panel). Self-gravity of the clump was turned off.

with an initial 1σ radius of 12 pc remains too compact to explain its present appearance (see Fig. 7). Therefore, we have examined the disruption timescale of a clump with 1σ radius of 35 pc, which is similar to the present extent of the clump. A compilation of the parameters for our reference model is given in Table 1. When clump’s self-gravity is taken into account, a velocity dispersion of 0.5 km s^{-1} is not enough to keep the clump in virial equilibrium and the clump collapses to a hotter compact configuration. In order to have the clump in a relaxed state, we needed to adjust the initial one-dimensional velocity dispersion.

Figures 8 and 9 show the evolution of the clump (assuming $\Upsilon_\star = 5.8$) on a near radial orbit and on circular orbit as those described in section 5.1 but including self-gravity in the REFE approximation. The initial one-dimensional velocity dispersion of the clump is 1 km s^{-1} . Although the disruption of the clump is slightly faster when the clump is on a near-radial orbit, dissolution of the clump occurs within 1.25 Gyr in both cases. When self-gravity is turned off, the cluster of stars is erased within 0.5 Gyr.

In order to gain more physical insight, we will focus on the simulation with the clump on circular orbit. The clump cannot be considered in isolation at any time because the mean internal acceleration due to mutual forces between the stars of the clump, $\langle g_{\text{int}} \rangle$, is initially $\simeq 0.9g_E$ and decreases in time as the stars of clump becomes more loosely bound. For instance, $\langle g_{\text{int}} \rangle$ averaged over all the simulated stars is $0.37g_E$ at $t = 0.5$ Gyr. In Fig. 10, the MOND boost factor $g_{\text{int}}/g_{\text{int,N}}$ at $t = 0.5$ Gyr is plotted as a function of the

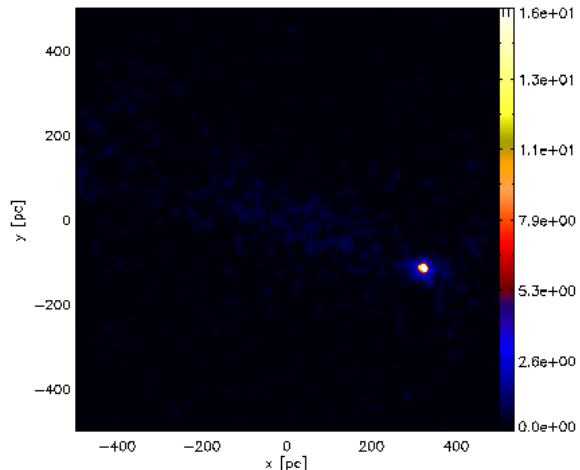


Figure 7. Stellar surface density in $M_\odot \text{ pc}^{-2}$ on the orbital plane after 6 Gyr, for a clump with initial 1σ radius of 12 pc, one-dimensional velocity dispersion of 1.8 km s^{-1} and a speed at apogalacticon equal to 0.07 times the circular speed. Self-gravity of the clump was included.

distance to clump’s centre. Once a star has been stripped away from the clump, at distances > 100 pc, it feels a constant boost factor and its dynamics is Newtonian but with a larger effective Newton constant G . All the particles lie in the quasi-Newtonian regime when the clump is erased.

Newtonian conservation laws such as the the conservation of the total energy and total angular momentum are only preserved in the REFE approximation when the dynamics of all the stars is quasi-Newtonian. In order to quantify the degree of conservation in our simulations, we have computed the net internal force $m \sum_N \mathbf{g}_{\text{int}}$ (being m the particle mass) summed over all the simulated particles and the total angular momentum. The net internal force fluctuates in time but it is always less than 0.5 percent the characteristic background force $M_{cl}v_{cc}^2/r_c$, where v_{cc} is the circular speed around UMi at r_c . The total angular momentum, on the other hand, increases by 4 percent during the first Gyr and by 0.5 percent between 1 Gyr and 1.5 Gyr. Therefore, the inspiraling of the clump from an initial radius of 390 pc to 355 pc at 1 Gyr (see Fig. 9) is not an artifact but the result of the gravitational transfer of angular momentum from the clump to the trailing tidal tail. We must also notice at this point that the density substructures displayed in the map at 1.5 Gyr do not have statistical significance, as Fig. 11 demonstrates.

A reduction of Υ_\star leads to an increase of the crossing time of the clump around UMi’s centre but also the mass of the clump is lowered if we assume that the clump has the same Υ_\star as the background stars. For $\Upsilon_\star = 2.2$ ($M_{cl} = 3 \times 10^4 M_\odot$), the clump dissolves within 1.25 Gyr as well because clump’s self-gravity is less relevant.

It may be worthwhile exploring whether the destruction timescale depends on the adopted value of the apocenter of the clump’s orbit. For an apogalactic distance of 750 pc, we find that the clump is erased in $\lesssim 1$ Gyr (see Fig. 12). Therefore, the persistence of the clump cannot be accounted for by altering its orbital parameters.

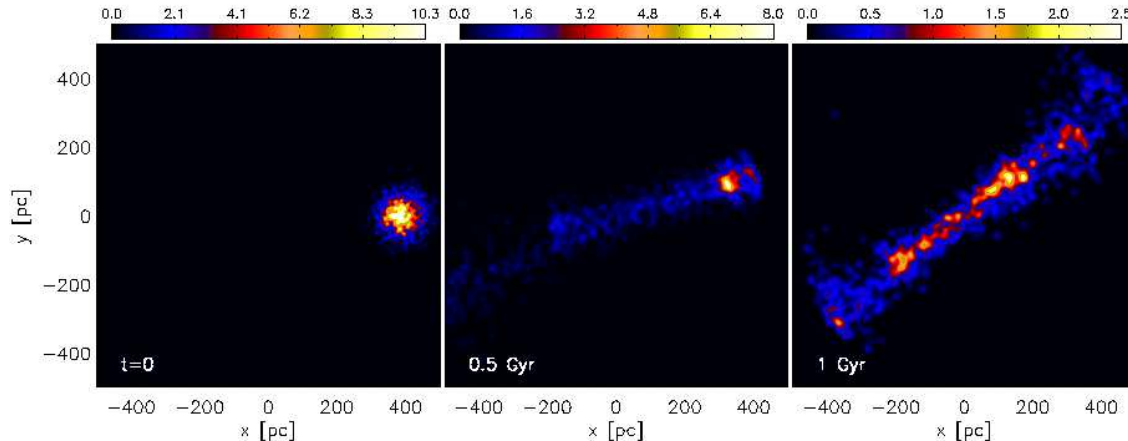


Figure 8. Evolution of the stellar surface density in $M_{\odot} \text{ pc}^{-2}$ for a clump with initial 1σ radius of 35 pc, one-dimensional velocity dispersion of 1 km s^{-1} and a speed at apogalacticon equal to 0.07 times the circular speed. Self-gravity of the clump was included.

Self-consistent simulations of the evolution of a low-mass satellite were carried out by Kroupa (1997) and Klessen & Kroupa (1998). They found that the unbound distinguishable remnant, consisting of particles with phase-space characteristics that reduce spreading along the orbit as those described by Kuhn (1993), contains a mass of about 1% of the initial mass of the progenitor. In the case of UMi’s clump, which has a mass of $\sim 7.8 \times 10^4 M_{\odot}$ for $\Upsilon_{\star} = 5.8$, the long-lived remnant should have a mass of $\sim 780 M_{\odot}$, too small to be detected in our simulations.

In all our previous REFE models, the external acceleration was taken as constant and equal to the instantaneous external acceleration of UMi at its current position. The external acceleration, however, may increase with time as UMi orbit penetrates deeper into the Milky Way halo when it moves towards pericentre. Piatek et al. (2005) measured the proper motion for UMi and found a perigalacticon and apogalacticon of 40 ± 36 kpc and 89 ± 71 kpc (at 95% confidence level), respectively. According to Eq. (8), as UMi plunges in on an eccentric orbit, it puffs up and expands adiabatically because g_I gets smaller at larger external accelerations (Brada & Milgrom 2000). Thus, the rotation timescale of the clump around UMi slows. For the same reason, the self-gravity of the clump lowers and the clump also inflates, rendering itself more susceptible to tidal dissolution. In other words, when the strength of the external acceleration increases, the internal accelerations, g_I and g_{int} , decrease. In Figure 13, we show snapshots of the surface density of the clump and its debris when UMi is on a non-circular orbit with apogalacticon and perigalacticon at 89 and 40 kpc, respectively. For our MOND value, $V_{\infty} = 170 \text{ km s}^{-1}$, the orbital period of UMi about the Galactic centre is 1.7 Gyr. In this simulation, UMi was also initially located at a galactocentric distance of 76 kpc and has negative velocity, i.e., it is approaching to the Galactic centre. The external acceleration increases until UMi reaches pericentre after 0.45 Gyr. An obvious consequence of the adiabatic expansion of UMi is that the orbit of the clump becomes more wide with time up to 0.45 Gyr. This can be seen clearly in the second panel of Fig. 13; the orbital radius is ~ 500 pc at $t = 0.5$ Gyr. By comparing Figs 9 and 13, we find that, at $t = 1$ Gyr,

the clump is able to retain more mass in the simulation in which UMi is placed on a non-circular orbit about the Milky Way but, still, the clump dissipates in < 1.5 Gyr. We can safely establish that the varying external acceleration felt by the dwarf because of its orbital motion does not offer a promising solution to the survival problem of the clump. On the contrary, Galactic tides, not included in our simulations, may help destroy the substructures if UMi’s orbit is very elongated (say, perigalacticon at < 25 kpc).

Our simulations have assumed that the mass distribution of UMi is spherical whereas the isophlets of UMi have ellipticities of 0.54. Since in MOND the gravity comes solely from the stellar component, the potential should be flatter, not spherical. A perfectly spherical potential has orbits that are confined to lie on planes. By contrast, orbits in axisymmetric potentials generally show precession of their orbital planes (except for exactly planar or exactly polar orbits), leading to an additional source of orbital mixing.

We have explored whether a flattened mass distribution, such as that observed in UMi, might change the slope of the rotation curve in the equatorial plane. In order to estimate this effect, we have modeled the stellar bulk of UMi as a flattened King model:

$$\rho(R, z) = \rho_K(m) \quad \text{with} \quad m^2 = R^2 + \frac{z^2}{\epsilon^2}, \quad (10)$$

where ρ_K is the density profile of the spherical King model, and derived numerically the circular velocity (see, e.g., §2.3 in Binney & Tremaine 1987). At radii $r < 0.6$ kpc, the UMi rotation curve in the equatorial plane is again a scaled-version of the curve derived in the spherical case. If we adopt the same central volume mass density as in the spherical case, and a flattening of $\epsilon = 0.54$, the amplitude of the Newtonian rotation curve decreases by a factor of 0.85. Therefore, if the clump is on a radial orbit in the equatorial plane of UMi, the inclusion of the ellipticity is similar to the use of a spherical model with $\Upsilon_{\star} = 4.2$. Given the uncertainties in Υ_{\star} , this is a secondary effect and a more accurate treatment of the flattening is not yet justified by the observations.

We conclude that the interpretation that the stellar clump is a dynamical fossil is difficult to sustain in MOND because its lifetime is less than ~ 1.5 Gyr even if clump’s

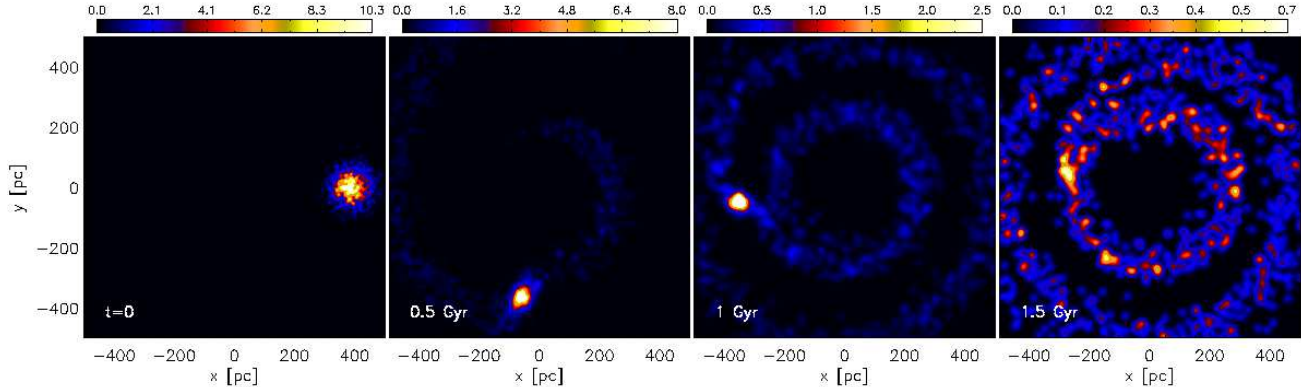


Figure 9. Stellar surface density in $M_{\odot} \text{pc}^{-2}$ of the debris for a clump on a circular orbit and initial 1σ radius of 35 pc and one-dimensional velocity dispersion of 1 km s^{-1} . Self-gravity of the clump was included.

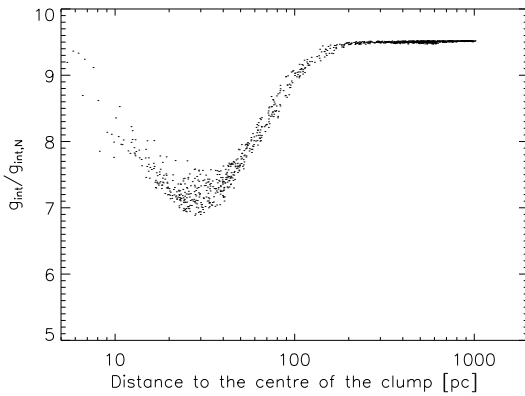


Figure 10. Internal acceleration boost for all the simulated stars as a function of the distance to the centre of the clump, at $t = 0.5$ Gyr, for the simulation shown in Fig. 9.

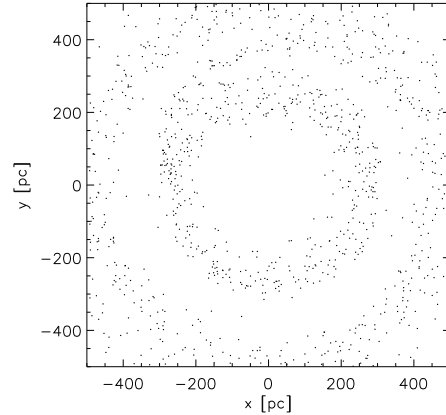


Figure 11. Distribution of the simulated stars at $t = 1.5$ Gyr for the model shown in Fig. 9.

self-gravity is taken into account. In the next section, we will discuss other scenarios and potential problems.

6 ALTERNATIVE SCENARIOS AND CAVEATS

In section 5, we consider the dissolution of an unbound clump, treating the background as a rigid potential. However, dynamical friction may induce a strong orbital decay of clusters in dSph galaxies. If the dark matter halo of UMi follows a NFW profile, clusters of mass $> 5 \times 10^4 M_{\odot}$ sink to the centre within one Hubble time if they are initially placed within 1 kpc from the dwarf galaxy centre (e.g., Goerdt et al. 2006; Sánchez-Salcedo et al. 2006; Peñarrubia et al. 2009). In the case of MOND, the orbital decay proceeds even faster (Sánchez-Salcedo et al. 2006; Nipoti et al. 2008). A fully satisfactory scenario should explain simultaneously the survival of the clump against phase-mixing and against orbital decay.

In the dark matter scenario, both problems are solved simultaneously if the dark matter halo has a core (Goerdt et al. 2006; Sánchez-Salcedo et al. 2006). In MOND, the clump can remain in orbit as long as its starting distance is

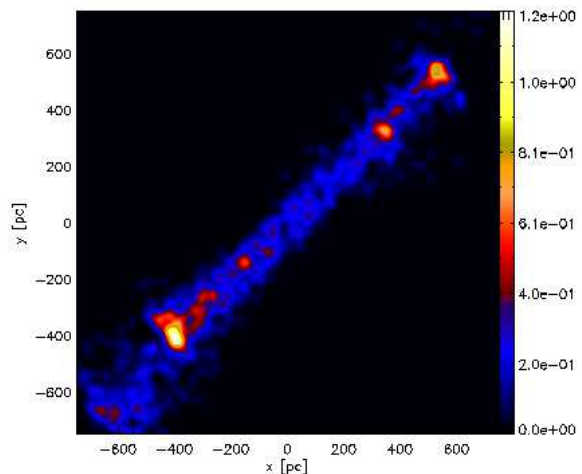


Figure 12. Tidal debris of a clump with apogalacticon at 750 pc and on near-radial orbit, at $t = 1$ Gyr. The clump has an initial 1σ radius of 35 pc and one-dimensional velocity dispersion of 1 km s^{-1} .

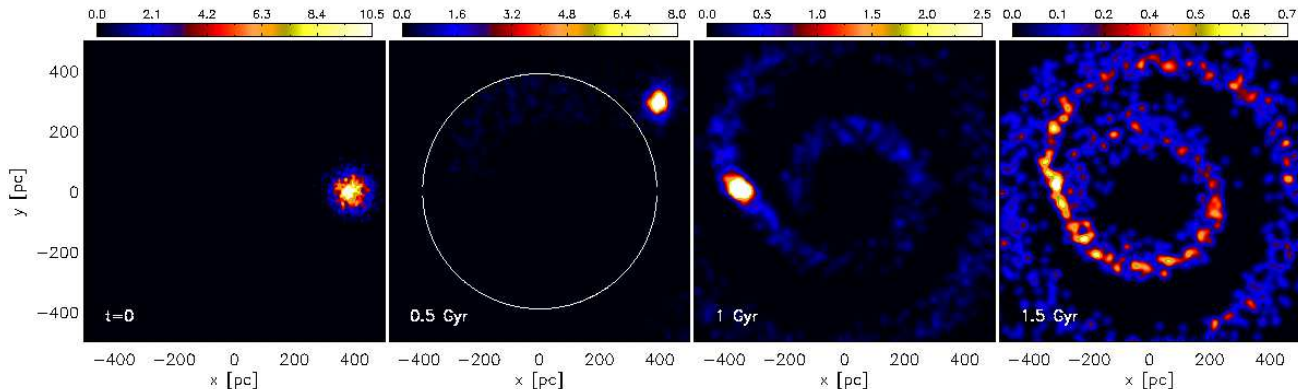


Figure 13. Stellar surface density in $M_{\odot} \text{pc}^{-2}$ of the debris assuming that the orbit of UMi around the Milky Way has the pericentre at 40 kpc and apocentre at 89 kpc. The galactocentric distances of UMi are $R_{gc} = (76, 41, 81, 86)$ kpc, at $t = (0, 0.5, 1.0, 1.5)$ Gyr, respectively. In this simulation, the initial clump has a 1σ radius of 35 pc and starts on a circular orbit of 390 pc radius, which is represented by a circle in the second panel. Self-gravity of the clump was included.

large enough so that the dynamical friction force is highly suppressed due to the low stellar density of the background (Angus & Diaferio 2009). As already discussed, the clump cannot survive against tidal diffusion even if its apocentre is placed at the tidal radius (~ 2 kpc), because the dissolution timescale depends on the gradients of the orbital frequencies (e.g., $d\Omega/dR$), which decay slowly with R .

It is important to consider other alternative scenarios for the presence of regions with cold density excess in dSph galaxies. It might be that the UMi’s clump is not a dynamical fossil but the disrupting remnant of a more massive globular cluster in the act of dispersing. Although this possibility requires a very fine-tuning of the initial parameters of the globular cluster and circularity of its orbit, it might be viable if the dark matter halo is cuspy because the density of dark matter towards the galactic centre might be sufficient to create a strong tidal field able to disrupt a globular cluster of mass $\lesssim 5 \times 10^4 M_{\odot}$ if it plunges close enough into the centre of the dwarf (Peñarrubia et al 2009).

In section 5.2, we saw that a compact clump with initial 1σ radius of 12 pc cannot be disrupted by galactic tides. Hence, a typical globular cluster of mass $\sim 0.8 \times 10^5 M_{\odot}$ is unaffected by the galactic tides in MOND, even if the orbit brings the cluster to the centre of the dwarf galaxy. This is expected because the mean density of a typical globular cluster is higher than the mean density of a dSph galaxy. Therefore, the clump could be a recently disrupted cluster which survived for a long time ($\gtrsim 10$ Gyr) due to being initially bound and *more massive*, if the parameters of the clump progenitor were fine-tuned to be initially much more tenuous and extended than a globular cluster. How massive should the progenitor be in this scenario? The cluster will be subject to a prolonged and slow mass-loss regime before it suffers from a sharp tidal disruption. Peñarrubia et al. (2002, 2009) and Zhao (2004) find that cored stellar systems lose 90 – 95 percent of its initial mass during the slow mass-loss regime. This implies that the progenitor should contain > 13 percent of the total mass of UMi. Clearly, this model presents severe inconsistencies because such a massive progenitor is expected to remain unaltered by tidal stirring. In

addition, it is difficult to explain why this cluster did not sink to the galaxy centre.

Another related possibility is that the stellar overdensity is not a distinct identity but a portion of a stationary large-scale structure. For instance, density cusps may emerge in the projection of eccentric discs (Tremaine 1995) or in the projection of the tidal debris of a disrupted stellar cluster in triaxial NFW systems (Peñarrubia et al. 2009). Since simulated cold substructures always show a symmetric pattern with respect to the dwarf centre, which has not been observed so far in the case of UMi’s clump, Peñarrubia et al. (2009) suggest that either a significant fraction of tidal debris remains undetected or that the origin of the clump is not related to the debris of a stellar cluster. In the particular case of UMi’s clump, it is unclear if, starting with a typical globular cluster, this model can explain simultaneously its high surface brightness and its low internal velocity dispersion (Peñarrubia et al. 2009). Moreover, the position of the resulting stellar substructures in the simulations of Peñarrubia et al. (2009) are localized at a projection distance from the galactic centre of 0.6 – 0.8 times the apocentre of progenitor’s orbit. Therefore, if we assume that the orbit of the progenitor in UMi is close to the plane of the sky, this constraint places the apocentre of the progenitor within two core radius, i.e. ~ 800 pc, which might be insufficient to prevent orbital decay of the putative progenitor by dynamical friction.

Wilkinson et al. (2004) suggested that the cold clump in UMi is a projection of a cold extratidal population onto the face of the dSph. Using numerical simulations, Read et al. (2006) explored this scenario in the standard Newtonian dark matter scenario and concluded that this hypothesis is falsified for two main reasons. First, there is always a source of hot tidal stars which mask any cold populations. Secondly, the population of stars beyond the tidal radius always appears hot in projection because there are more stars on circular orbits than radial orbits at the tidal radius. Since we cannot see a reason to believe that these arguments cannot be applied in MOND, we conclude that if such cold clump is real, it could not have formed as a result of tidal effects.

7 CONCLUSIONS

Observations of the rotation curves of spiral galaxies strongly support a one-to-one relation between gravity at any radius and the enclosed baryonic mass. Due to this empirical relation, modified gravity theories like MOND are able to account rather successfully for the amplitude and the shape of the rotation curves. There are some indirect phenomena that suggest that this empirical relation may break down at scales of dSph galaxies (e.g., Gilmore et al. 2007, and references therein), challenging the interpretation of a modification of gravity as a substitute for dark matter.

Localized regions with enhanced stellar density and, where data permit, extremely cold kinematics have been detected in some dSph galaxies (e.g., Olszewski & Aaronson 1985; K03; Coleman et al. 2004; Walker et al. 2006). In the framework of CDM, K03 show that adopting a cored halo profile can preserve the UMi's clump incorrupted for a Hubble time. This cored halo can fit the observed stellar velocity dispersion and the persistence of the clump. However, although we are still unable to make robust predictions about how the dark matter distribution changes in the process of galaxy formation when the physics of baryons are included, the formation of a large core in a dark matter dominated galaxy, provides a hard challenge for Λ CDM. Mashchenko et al. (2008) showed that energy feedback in dwarf galaxies drives bulk gas motions and gravitational potential fluctuations large enough to turn the cusp into a flat core (see also Governato et al. 2009). They find that for a Fornax sized galaxy, the dark matter core has an average density of $0.2M_{\odot} \text{ pc}^{-3}$ at redshift $z = 5.2$, and the density decays a factor $\sqrt{2}$ in ~ 300 pc. Still, such a core would not be enough to avoid orbital spreading of the clump.

In the particular case of UMi dSph galaxy, the density excess around the secondary peak cannot be the remnant of a merger with UMi of a smaller, gas-rich system because the stars have the same properties in terms of color and magnitude as the body of the UMi population (Kleyna et al. 1998). One might wonder whether the density peak could instead be a projection effect and that what we are seeing is a cold, low-density tidal tail. Numerical experiments by Read et al. (2006) have shown that this scenario is very unlikely. Another possibility is that the clump is a portion of the stationary debris of a disrupted globular cluster. This model is not implausible but cannot be proven yet.

A more drastic alternative scenario consists in interpreting the survival of substructures as an internal inconsistency of Λ CDM. We have explored if MOND can explain the longevity of unbound clumps in dSph galaxies. Following K03, we have assumed that this overdensity structure is a disrupted stellar cluster and simulate its evolution in the gravitational potential derived in MOND. Whichever the form of the orbit, the clump is tidally disrupted within 1.5 Gyr, even if clump's self-gravity is included. One can decrease UMi mass by adopting a smaller Υ_{*} , slowing the process of orbital mixing because the crossing time for the clump becomes larger. However, even assuming a mass-to-light ratio of $0.8M_{\odot}/L_{\odot}^V$, the clump is disrupted in < 2.5 Gyr. Our conclusion that tidal forces should have disrupted the clump appears robust for the adopted value of the stellar mass-to-light ratio of UMi.

The external field acceleration felt by UMi from the

Milky Way depends on the galactocentric distance of UMi, which is time dependent if the orbit of UMi around the Galactic halo is elongated. However, the temporal variation of the EFE can hardly boost the longevity of the clump.

In the absence of any alternative model to explain the origin of the cold clump, we conclude that it is challenging for both Λ CDM and MOND to explain the nature and dynamics of the clump in UMi. Another alternative of gravity suggested by Moffat (2005) is the so-called Modified Gravity (MOG). It is a fully covariant theory which predicts a Yukawa-like modification of Newton's law. For a system with a baryonic mass of a few times $10^6 M_{\odot}$ like UMi dSph galaxy, MOG predicts little or no observable deviation from Newtonian gravity at galactic distances of ~ 200 pc (e.g., Moffat & Toth 2008). Therefore, explaining the internal dynamics of dSph galaxies is problematic without advocating dark matter, weakening the appeal of the MOG model. Other authors achieve to find modified theories of gravity which seem to reproduce the rotation curves of galaxies (e.g., Capozziello et al. 2007). Nevertheless, an analysis of the dynamics of dSph galaxies in these theories is still missing.

ACKNOWLEDGMENTS

We warmly thank our referee for constructive comments and valuable suggestions that helped us improve this paper. We are grateful to A. Esquivel, J. Magaña, A. Rodríguez and O. Valenzuela for useful comments. We gratefully acknowledge support from CONACyT project CB-2006-60526 and PAPIIT IN114107.

REFERENCES

- Angus, G. W. 2008, MNRAS, 387, 1481
- Angus, G. W., & Diaferio, A. 2009, MNRAS, 396, 887
- Angus, G. W. & McGaugh, S. S. 2008, MNRAS, 383, 417
- Bekenstein, J., & Milgrom, M. 1984, ApJ, 286, 7
- Bellazzini, M., Ferraro, F. R., Origlia, L., Pancino, E., Monaco, L., & Olivia, E., 2002, AJ, 124, 3222
- Binney, J., & Tremaine, S. 1987, Galactic Dynamics (Princeton Series in Astrophysics)
- Brada, R., & Milgrom, M. 1995, MNRAS, 276, 453
- Brada, R., & Milgrom, M. 2000, ApJ, 541, 556
- Chandrasekhar, S. 1942, Principles of Stellar Dynamics (University of Chicago Press)
- Capozziello, S., Cardone, V. F., & Troisi, A. 2007, MNRAS, 375, 1423
- Carrera, R., Aparicio, A., Martínez-Delgado, D., & Alonso-García, J. 2002, AJ, 123, 3199
- Coleman, M., Da Costa, G. S., Bland-Hawthorn, J., Martínez-Delgado, D., Freeman, K. C., & Malin, D. 2004, AJ, 127, 832
- Demers, S., Battinelli, P., Irwin, M. J., & Kunkel, W. E. 1995, MNRAS, 274, 491
- Eskridge, P. B., & Schweitzer, A. E. 2001, AJ, 122, 3106
- Famaey, B., & Binney, J. 2005, MNRAS, 363, 603
- Fellhauer, M., & Heggge, D. C. 2005, A&A, 435, 875
- Gentile, G., Famaey, B., Combes, F., Kroupa, P., Zhao, H. S., & Tiret, O. 2007, A&A, 472, L25
- Gerhard, O. E., & Spergel, D. N. 1992, ApJ, 397, 38
- Gilmore, G., Wilkinson, M. I., Wyse, R. F. G., Kleyna, J. T., Koch, A., Evans, N. W., & Grebel, E. K. 2007, ApJ, 663, 948
- Goerdt, T., Moore, B., Read, J. I., Stadel, J., & Zemp, M. 2006, MNRAS, 368, 1073

Governato, F., et al. 2009, arXiv:0911.2237
 Hayashi, E., et al. 2003, ApJ, 584, 541
 Irwin, M., & Hatzidimitriou, D. 1995, MNRAS, 277, 1354
 Keenan, D. W. 1981a, A&A, 95, 334
 Keenan, D. W. 1981b, A&A, 95, 340
 Klessen, R. S., & Kroupa, P. 1998, ApJ, 498, 143
 Kleyna, J. T., Geller, M. J., Kenyon, S. J., Kurtz, M. J., & Thorstensen, J. R. 1998, ApJ, 115, 2359
 Kleyna, J. T., Wilkinson, M. I., Gilmore, G., & Evans, N. W. 2003, ApJ, 588, L21 (K03)
 Kroupa, P. 1997, New Astron., 2, 139
 Kroupa, P., Theis, C., & Boily, C. M. 2005, A&A, 431, 517
 Kuhn, J. R. 1993, ApJ, 409, L13
 Llinares, C., Knebe, A., Zhao, H. 2008, MNRAS, 391, 1778
 Lokas, E., Mamon, G., & Prada, F. 2006, EAS Publications Series, Volume 20, 113
 Lora, V., Sánchez-Salcedo, F. J., Raga, A. C., & Esquivel, A. 2009, ApJ, 699, L113
 Mapelli, M., Ripamonti, E., Tolstoy, E., Sigurdsson, S., Irwin, M. J., & Battaglia, G. 2007, MNRAS, 380, 1127
 Mashchenko, S., Wadsley, J., & Couchman, H. M. P. 2008, Science, 319, 174
 Milgrom, M. 1983, ApJ, 270, 365
 Milgrom, M. 1986, ApJ, 302, 617
 Milgrom, M. 1995, ApJ, 455, 439
 Milgrom, M., & Sanders, R. H. 2006, ApJ, 658, L17
 Moffat, J. W. 2005, J. Cosmol. Astropart. Phys., 505, 3
 Moffat, J. W., & Toth, V. T. 2008, ApJ, 680, 1158
 Muñoz, R. R., et al. 2005, ApJ, 631, L137
 Nipoti, C., Ciotti, L., Binney, J., & Londrillo, P. 2008, MNRAS, 386, 2194
 Olszewski, W. W., & Aaronson, M. 1985, AJ, 90, 2221
 Oort, J. H. 1965, in Stars and Stellar Systems, 5, Galactic Structure, ed. A. Blaauw & M. Schmidt (University of Chicago Press), 455
 Palma, C., Majewski, S. R., Siegel, M. H., Patterson, R. J., Osthheimer, J. C., & Link, R. 2003, AJ, 125, 1352
 Peñarrubia, J., Kroupa, P., Boily, C. M. 2002, MNRAS, 333, 779
 Peñarrubia, J., Navarro, J. F., & McConnachie, A. W. 2008, ApJ, 673, 226
 Peñarrubia, J., Walker, M. G., & Gilmore, G. 2009, MNRAS, 399, 1275
 Piatek, S., et al. 2008, AJ, 130, 95
 Read, J. I., Wilkinson, M. I., Evans, N. W., Gilmore, G., & Kleyna, J. T. 2006, MNRAS, 367, 387
 Sánchez-Salcedo, F. J. 2009, MNRAS, 392, 1573
 Sánchez-Salcedo, F. J., & Hernandez, X. 2007, ApJ, 667, 878
 Sánchez-Salcedo, F. J., Reyes-Iturbide, J., & Hernandez, X. 2006, MNRAS, 370, 1829
 Sanders, R. H., & McGaugh, S. S. 2002, ARA&A, 40, 263
 Sanders, R. H., & Noordermeer, E. 2007, MNRAS, 379, 702
 Stoehr, F., White, S. D. M., Tormen, G., & Springel, V. 2002, MNRAS, 335, L84
 Trachternach, C., de Blok, W. J. G., Walter, F., Brinks, E., & Kennicutt, R. C. 2008, AJ, 136, 2720
 Tremaine, S. 1995, AJ, 110, 628
 Walker, M. G., Mateo, M., Olszewski, E. W., Pal, J. K., Sen, B., & Woodroffe, M. 2006, ApJ, 642, L41
 Walker, M. G., Mateo, M., Olszewski, E. W., Peñarrubia, J., Evans, N. W., & Gilmore, G. 2009, arXiv: 0906.0341
 Wielen, R. 1977, A&A, 60, 263
 Wilkinson, M. I., Kleyna, J. T., Evans, N. W., Gilmore, G. F., Irwin, M. J., & Grebel, E. K. 2004, ApJ, 611, L21
 Wu, X., Zhao, H. S., Famaey, B., Gentile, G., Tirez, O., Combes, F., Angus, G. W., & Robin, A. C. 2007, ApJ, 665, L101
 Zhao, H. 2004, MNRAS, 351, 891
 Zhao, H. S. 2005, A&A, 444, L25
 Zhao, H., & Tian, L. 2006, A&A, 450, 1005

APPENDIX A: MODIFIED EPICYCLES OF STARS IN AN UNBOUND SYSTEM IN MOND

Fellhauer & Heggie (2005) studied the evolution of an idealized unbound system in a tidal field. In this Appendix, we extend the theory to MOND. The reader is referred to Fellhauer & Heggie (2005) for a discussion about the limitations of the theoretical model.

We consider a small and unbound system on a circular orbit with radius R_0 in the axisymmetric potential of its host galaxy. Therefore, the clump is embedded in the external field created by the galaxy Φ_e . We use rotating, cluster-centred coordinates ξ , ζ and z . The ξ -axis points to the anticentre of the galaxy, and the ζ -axis points in the direction of orbital motion of the clump. The presence of the clump will change the gravitational potential by some increment Φ_i , i.e. $\Phi = \Phi_e + \Phi_i$. If Φ_i can be treated as a perturbation, the gravitational field equation that governs the kinematics is

$$\left(\nabla^2 + L_0 \frac{\partial^2}{\partial \xi^2}\right) \Phi_i = 4\pi\mu_0^{-1}G\rho \quad (\text{A1})$$

(Milgrom 1986). Here ρ is the density of the clump, $\mu_0 \equiv \mu(|\nabla\Phi_e|/a_0)$ and L_0 is the logarithmic derivative of μ_0 (in the unperturbed system).

We adopt an equilibrium model in which stars are distributed uniformly within a triaxial ellipsoid and whose epicycles are centered at the centre of the ellipsoid. The equations of stellar motion in the epicyclic approximation (e.g., Chandrasekhar 1942) are given by

$$\ddot{\xi} - 2\Omega\dot{\zeta} - 4\Omega A\xi = -\frac{\partial\Phi_i}{\partial\xi}, \quad (\text{A2})$$

$$\ddot{\zeta} + 2\Omega\dot{\xi} = -\frac{\partial\Phi_i}{\partial\zeta}, \quad (\text{A3})$$

$$\ddot{z} + \nu^2 z = -\frac{\partial\Phi_i}{\partial z}, \quad (\text{A4})$$

where ξ , ζ and z are the deviations of the stellar orbit from the circular guiding centre. Here ν is the vertical frequency, $\nu^2 = \partial^2\Phi_e/\partial z^2$, and A is the Oort constant

$$A = -\frac{1}{2} \left(R \frac{d\Omega}{dR} \right)_{R_0}. \quad (\text{A5})$$

Following Fellhauer & Heggie (2005), it is possible to construct a distribution of epicyclic amplitudes so that the space density is uniform within a triaxial ellipsoid with semi-major axes a , αa and a/Λ_0 , where $a > 0$ is a free parameter that specifies the size of the clump, $\Lambda_0 \equiv \sqrt{1 + L_0}$, and α will be determined from the shape of closed epicycles. The field equation (A1) for Φ_i can be transformed into the standard Poisson equation by making the substitution $\xi' = \xi/\Lambda_0$. The resultant equation can be written as

$$\tilde{\nabla}^2 \Phi'_i = 4\pi\mu_0^{-1}G\rho(\Lambda_0\xi', \zeta, z), \quad (\text{A6})$$

where $\Phi'_i = \Phi'_i(\xi', \zeta, z)$ and $\tilde{\nabla}^2 = \partial^2/\partial\xi'^2 + \partial^2/\partial\zeta^2 + \partial^2/\partial z^2$. Therefore, Φ'_i is the Newtonian potential created by an ellipsoid of constant density ρ/μ_0 , bounded by the surface $a^2 = \Lambda_0^2(\xi'^2 + z^2) + \zeta^2/\alpha^2$, which is a prolate ellipsoid with eccentricity $e' = \sqrt{1 - (\Lambda_0\alpha)^{-2}}$. Taking advantage of the theory of homeoids, $\Phi' = \pi G\mu_0^{-1}A'_1\rho(\xi'^2 + z^2) + \pi G\mu_0^{-1}\rho A'_3\zeta^2$, where $A'_1 = A_1(e')$ and $A'_3 = A_3(e')$ are given in Table 2-1

of Binney & Tremaine (1987). Therefore, Equations (A2)-(A4) can be written in terms of $B'_1 = 2\pi G\rho A'_1/(\Lambda_0^2\mu_0)$ and $B'_3 = 2\pi G\rho A'_3/\mu_0$ as

$$\ddot{\xi} - 2\Omega\dot{\zeta} + (\kappa^2 - 4\Omega^2)\xi = -B'_1\xi, \quad (\text{A7})$$

$$\ddot{\zeta} + 2\Omega\dot{\xi} = -B'_3\zeta, \quad (\text{A8})$$

$$\ddot{z} + \nu^2 z = -\Lambda_0^2 B'_1 z, \quad (\text{A9})$$

where κ is the epicyclic frequency if the clump itself is neglected. As shown by Fellhauer & Heggie (2005), the epicycle frequency and the vertical frequency are altered by the self-gravity of clump:

$$\kappa_{\pm}'^2 = \frac{1}{2} \left(\kappa^2 + B'_1 + B'_3 \pm \sqrt{(\kappa^2 + B'_1 - B'_3)^2 + 16\Omega^2 B'_3} \right), \quad (\text{A10})$$

and

$$\nu'^2 = \nu^2 + \Lambda_0^2 B'_1. \quad (\text{A11})$$

If we choose the lower sign for κ' in Eq. (A10), there exist exponentially growing solutions (i.e. $\kappa'^2 < 0$) provided that

$$R \frac{d\Omega^2}{dR} < -B'_1. \quad (\text{A12})$$

In terms of density, one of the normal frequencies is imaginary when ρ is smaller than a certain critical density ρ_{cr} ,

$$\rho < \rho_{\text{cr}} \equiv \frac{\Lambda_0^2 \mu_0}{2\pi G A'_1} R \left| \frac{d\Omega^2}{dR} \right|. \quad (\text{A13})$$

If this condition is fulfilled, the complete solution is a linear combination of oscillatory solutions with frequency κ'_+ (those obtained by taking the upper sign for κ') and exponentially growing solutions:

$$\xi(t) = \xi_0 \cos(\kappa'_+ t + \psi_0) + \lambda \exp(kt), \quad (\text{A14})$$

$$\zeta(t) = -\alpha \xi_0 \sin(\kappa'_+ t + \psi_0) - \lambda R \exp(kt), \quad (\text{A15})$$

$$z(t) = z_0 \cos(\nu t + \psi_1), \quad (\text{A16})$$

where ξ_0 , z_0 , ψ_0 , ψ_1 and λ are free parameters, $k > 0$ is the imaginary part of κ'_- ,

$$\alpha = \frac{2\Omega\kappa'_+}{\kappa'^2_+ - B'_3}, \quad (\text{A17})$$

and

$$R = \frac{2\Omega k}{k^2 + B'_3}. \quad (\text{A18})$$

The equations for the epicyclic motions in the Newtonian case are naturally recovered from the above equations just by taking $\mu_0 = 1$ and $L_0 = 0$ (so that $\Lambda_0 = 1$). Due to the enhanced self-gravity of the clump by a factor of μ_0^{-1} in MOND, ρ_{cr} is smaller than in the equivalent Newtonian galaxy, i.e. the galaxy with additional dark matter that has the same $\Omega(R)$. In the particular case that ρ is much smaller than the critical density, we have:

$$k^2 \simeq \left(\frac{4\Omega^2}{\kappa^2} - 1 \right) B'_3. \quad (\text{A19})$$

We see that the dissolution time for very small initial density is $\propto \sqrt{B'_3} \propto \mu_0^{0.5} \rho^{-0.5}$ in the epicyclic approximation, which is valid for small clumps. Since $\mu_0 \leq 1$, the dissolution time is shorter in MOND than in its equivalent Newtonian galaxy. If the gravitational potential in which the clump is embedded

is harmonic, we have $\Omega(R) = \Omega_0$ and $\kappa = 2\Omega$, then $\rho_{\text{cr}} = 0$ and $k = 0$, implying that the dissolution time is infinite. This case was already discussed in in terms of the tidal radius in section 2.